

Impact of the recent measurements of the top-quark and W-boson masses on electroweak precision fits

J. de Blas,¹ M. Pierini,² L. Reina,³ and L. Silvestrini⁴

¹CAFPE and Departamento de Física Teórica y del Cosmos,
Universidad de Granada, Campus de Fuentenueva, E-18071 Granada, Spain

²CERN, 1211 Geneva 23, Switzerland

³Physics Department, Florida State University,
Tallahassee, FL 32306-4350, USA

⁴INFN, Sezione di Roma, Piazzale A. Moro 2, I-00185 Roma, Italy

We assess the impact of the very recent measurement of the top-quark mass by the CMS Collaboration [1] on the fit of electroweak data in the Standard Model and beyond, with particular emphasis on the prediction for the mass of the W boson. We then compare this prediction with the average of the corresponding experimental measurements including the new measurement by the CDF Collaboration [2], and discuss its compatibility in the Standard Model, in new physics models with oblique corrections, and in the dimension-six Standard Model Effective Field Theory. Finally, we present the updated global fit to electroweak precision data in these models.

The mass of the top quark (m_t) plays a crucial role in the study of Standard Model (SM) predictions for precision observables in the ElectroWeak (EW) and flavour sectors, since several amplitudes are quadratically sensitive to m_t . Indeed, indirect bounds on the top-quark mass were obtained using EW and flavour observables well before its direct measurement [3, 4]. Nowadays, m_t gives the dominant parametric uncertainty on several EW Precision Observables (EWPO) [5], among which is the W -boson mass (M_W). The posterior from a global fit omitting or including the experimental information on m_t and M_W is reported in Figure 1. (We also show in the same figure analogous information in the $\sin^2 \theta_{\text{eff}}^{\text{lep}}$ vs. M_W plane.) All posteriors reported in this paper are obtained from a Bayesian analysis performed with the HEPfit code [6], using state-of-the-art calculations for all EWPO¹ [7–37]. All inputs used are reported in Table II, while the theory uncertainties we use are:

$$\begin{aligned} \delta_{\text{th}} M_W &= 4 \text{ MeV}, & \delta_{\text{th}} \sin^2 \theta_W &= 5 \cdot 10^{-5}, & (1) \\ \delta_{\text{th}} \Gamma_Z &= 0.4 \text{ MeV}, & \delta_{\text{th}} \sigma_{\text{had}}^0 &= 6 \text{ pb}, \\ \delta_{\text{th}} R_\ell^0 &= 0.006, & \delta_{\text{th}} R_c^0 &= 0.00005, & \delta_{\text{th}} R_b^0 &= 0.0001. \end{aligned}$$

From Figure 1 it is evident that m_t and M_W are tightly correlated in the SM, so that experimental improvements in either one might challenge the validity of the SM and provide us with precious hints on what kind of New Physics (NP) might be present at yet unprobed energy scales. Indeed, this is precisely the situation once the very recent measurement of m_t from the CMS Collaboration [1],

$$m_t = 171.77 \pm 0.38 \text{ GeV}, \quad (2)$$

and of M_W from the CDF Collaboration [2],

$$M_W = 80.4335 \pm 0.0094 \text{ GeV}, \quad (3)$$

are included in the analysis. This Letter is dedicated to assessing the impact of these measurements in the SM and in several parametrizations of physics beyond the SM.

Let us first consider the impact of the new measurement of m_t in Eq. (2). Following Ref. [5], we combine the 2016 Tevatron combination [38], the 2015 CMS Run 1 combination [39], the combination of ATLAS Run 1 results in Ref. [40], the CMS Run 2 measurements in the dilepton, lepton+jets, all-jet and single-top channels [1, 41–43] and the ATLAS Run 2 result from the lepton+jet channel [44], assuming the linear correlation coefficient between two systematic uncertainties to be written as $\rho_{ij}^{\text{sys}} = \min \{ \sigma_i^{\text{sys}}, \sigma_j^{\text{sys}} \} / \max \{ \sigma_i^{\text{sys}}, \sigma_j^{\text{sys}} \}$. In this way we obtain a new average (compared to Ref. [5]) given by:

$$m_t = 171.79 \pm 0.38 \text{ GeV}, \quad (4)$$

where the uncertainty is dominated, as expected, by the very recent CMS measurement. However, since this average does not take into account the tensions between individual measurements, we also consider a *conservative average* in which the error is inflated to 1 GeV.

For the W -boson mass, we compute the average of all the existing measurements from LEP 2, the Tevatron, and the LHC. The new measurement from CDF gives, when combined with the D0 one, a Tevatron combination of $(80.427 \pm 0.0089) \text{ GeV}$ [2]. This was combined with the LHC ATLAS [45] and LHCb [46] measurements assuming a common systematic uncertainty of 4.7 MeV, corresponding to the CDF uncertainty from PDF and QED radiation. The resulting number is combined in an uncorrelated manner with the LEP2 determination, obtaining as new average:²

$$M_W = 80.4133 \pm 0.0080 \text{ GeV}. \quad (5)$$

¹ A thorough description of all elements entering the EWPO global fit used in this Letter is given in Ref. [5], to which we refer the reader interested in such details.

² We observe that the result of the combination does not depend strongly on the value of the common uncertainty between 0 and

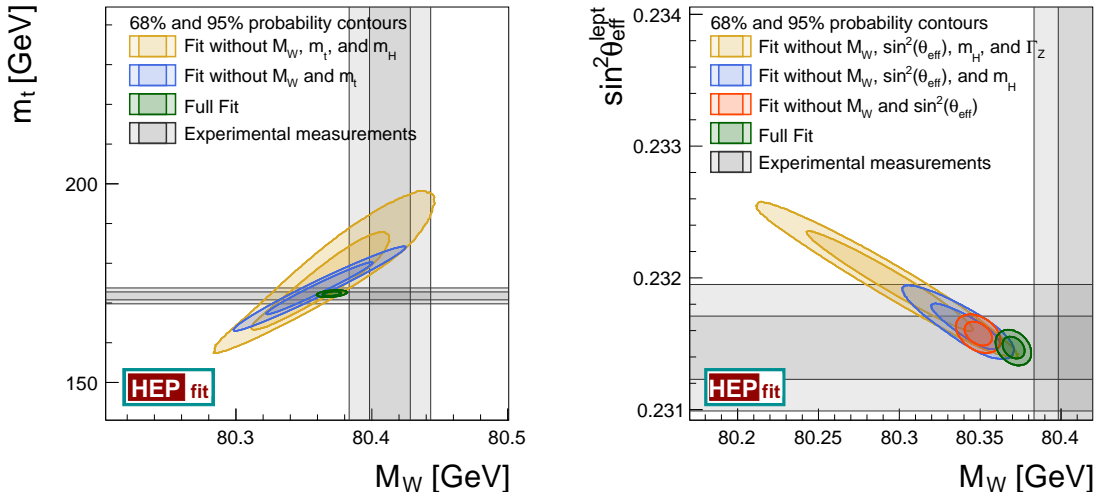


FIG. 1. Posterior from a global fit of all EWPO in the SM in the m_t vs. M_W (top) and $\sin^2 \theta_{\text{eff}}^{\text{lept}}$ vs. M_W (bottom) planes, superimposed to the posteriors obtained omitting different observables from the fit in the *standard average* scenario. Dark (light) regions correspond to 68% (95%) probability ranges. Direct measurements are shown in grey. The corresponding results in the *conservative average* scenario are presented in Figure 3.

As in the top-quark mass case, there is however a significant tension between the new CDF measurement and the other measurements that enter in the calculation of Eq. (5), with $\chi^2/n_{\text{dof}} = 3.59$. Therefore, in a *conservative average*, we inflate the error on M_W to 0.015 GeV.

We then perform a series of fits to the different EWPO using both the *standard* (see Eqs. 4 and 5) and *conservative* assumptions for the uncertainties of the top-quark and W -boson masses.³ (Although we will discuss both scenarios throughout the text, in most of the tables and figures in the main text we will report the results pertaining to the *standard average*. The results for the *conservative average* scenario are shown in the appendix.) In particular, we are interested in comparing the new averages with the corresponding predictions obtained in the SM. For that purpose we first perform a pure SM fit of all EWPO, excluding the experimental input for M_W and, from the posterior of such fit, we compute the SM prediction for M_W . The results are shown in Table I, where we also compare with the combined M_W values in each scenario via the 1D pull, computed as explained in Ref. [5]. As it is apparent, there exists a significant 6.5σ

discrepancy with the SM in the *standard average*, which persists at the level of 3.7σ even in the *conservative* scenario, due to the large difference between the new CDF measurement and the SM prediction.

Model	Pred. M_W [GeV] <i>standard average</i>	Pull	Pred. M_W [GeV] <i>conservative average</i>	Pull
SM	80.3499 ± 0.0056	6.5σ	80.3505 ± 0.0077	3.7σ
ST	80.366 ± 0.029	1.6σ	80.367 ± 0.029	1.4σ
STU	80.32 ± 0.54	0.2σ	80.32 ± 0.54	0.2σ
SMEFT	80.66 ± 1.68	-0.1σ	80.66 ± 1.68	-0.1σ

TABLE I. Predictions and pulls for M_W in the SM, in the *oblique* NP models and in the SMEFT, using the *standard* and *conservative* averaging scenarios. The predictions are obtained without using the experimental information on M_W . See text for more details.

In Tables II and VI we present, in addition to the experimental values for all EWPO used, the posterior from the global fit, the prediction of individual parameters/observables obtained omitting the corresponding experimental information, the indirect determination of SM parameters obtained solely from EWPO, and the full prediction obtained using only the experimental information on SM parameters. For the individual prediction, indirect determination and for the full prediction we also report the pull for each experimental result. In this regard, from the individual indirect determination of the SM parameters in Table II, one can observe how the tensions introduced by the new measurements in the SM fit result into sizable pulls for the different SM inputs, at the level of 4σ (6σ) for $\Delta\alpha_{\text{had}}^{(5)}(M_Z)$ and m_H (M_Z and m_t). Each pull can be converted in a p -value, and the global consistency of the SM in the EWPO domain can

6.9 MeV, the total CDF systematic uncertainty [2]. In particular, the combined uncertainty ranges between 7.7 and 8.4 MeV, whereas the central values can change by slightly less than 1σ . Thus, waiting for an official combination of LHC and Tevatron results, we take the result in Eq. 5 as our best estimate of M_W .

³ Unlike in Ref. [5], we do not consider an inflated uncertainty for the Higgs-boson mass in the *conservative* scenario since, as noted in that reference, this has little impact on the output of the EW fit. We thus use $m_H = (125.21 \pm 0.12)$ GeV in all the fits presented here.

	Measurement	Posterior	Indirect/Prediction	Pull	Full Indirect	Pull	Full Prediction	Pull
$\alpha_s(M_Z)$	0.1177 ± 0.0010	0.11762 ± 0.00095 [0.11576, 0.11946]	0.11685 ± 0.00278 [0.11145, 0.12233]	0.3	0.12181 ± 0.00470 [0.1126, 0.1310]	-0.8	0.1177 ± 0.0010 [0.1157, 0.1197]	-
$\Delta\alpha_{\text{had}}^{(5)}(M_Z)$	0.02766 ± 0.00010	0.027535 ± 0.000096 [0.027349, 0.027726]	0.026174 ± 0.000334 [0.025522, 0.026826]	4.3	0.028005 ± 0.000675 [0.02667, 0.02932]	-0.5	0.02766 ± 0.00010 [0.02746, 0.02786]	-
M_Z [GeV]	91.1875 ± 0.0021	91.1911 ± 0.0020 [91.1872, 91.1950]	91.2314 ± 0.0069 [91.2178, 91.2447]	-6.1	91.2108 ± 0.0390 [91.136, 91.288]	-0.6	91.1875 ± 0.0021 [91.1834, 91.1916]	-
m_t [GeV]	171.79 ± 0.38	172.36 ± 0.37 [171.64, 173.09]	181.45 ± 1.49 [178.53, 184.42]	-6.3	187.58 ± 9.52 [169.1, 206.1]	-1.7	171.80 ± 0.38 [171.05, 172.54]	-
m_H [GeV]	125.21 ± 0.12	125.20 ± 0.12 [124.97, 125.44]	93.36 ± 4.99 [82.92, 102.89]	4.3	247.98 ± 125.35 [100.8, 640.4]	-0.9	125.21 ± 0.12 [124.97, 125.45]	-
M_W [GeV]	80.4133 ± 0.0080	80.3706 ± 0.0045 [80.3617, 80.3794]	80.3499 ± 0.0056 [80.3391, 80.3610]	6.5	80.4129 ± 0.0080 [80.3973, 80.4284]	0.1	80.3496 ± 0.0057 [80.3386, 80.3608]	6.5
Γ_W [GeV]	2.085 ± 0.042	2.08903 ± 0.00053 [2.08800, 2.09006]	2.08902 ± 0.00052 [2.08799, 2.09005]	-0.1	2.09430 ± 0.00224 [2.0900, 2.0988]	-0.2	2.08744 ± 0.00059 [2.08627, 2.08859]	0.0
$\sin^2 \theta_{\text{eff}}^{\text{lept}}(Q_{\text{FB}}^{\text{had}})$	0.2324 ± 0.0012	0.231471 ± 0.000055 [0.231362, 0.231580]	0.231469 ± 0.000056 [0.231361, 0.231578]	0.8	0.231460 ± 0.000138 [0.23119, 0.23173]	0.8	0.231558 ± 0.000062 [0.231436, 0.231679]	0.7
$P_\tau^{\text{pol}} = \mathcal{A}_\ell$	0.1465 ± 0.0033	0.14742 ± 0.00044 [0.14656, 0.14827]	0.14744 ± 0.00044 [0.14657, 0.14830]	-0.3	0.14750 ± 0.00108 [0.1454, 0.1496]	-0.3	0.14675 ± 0.00049 [0.14580, 0.14770]	-0.1
Γ_Z [GeV]	2.4955 ± 0.0023	2.49455 ± 0.00065 [2.49329, 2.49581]	2.49437 ± 0.00068 [2.49301, 2.49569]	0.5	2.49530 ± 0.00204 [2.4912, 2.4993]	0.0	2.49397 ± 0.00068 [2.49262, 2.49531]	0.6
σ_h^0 [nb]	41.480 ± 0.033	41.4892 ± 0.0077 [41.4741, 41.5041]	41.4914 ± 0.0080 [41.4757, 41.5070]	-0.3	41.4613 ± 0.0303 [41.402, 41.521]	0.4	41.4923 ± 0.0080 [41.4766, 41.5081]	-0.4
R_ℓ^0	20.767 ± 0.025	20.7487 ± 0.0080 [20.7329, 20.7645]	20.7451 ± 0.0087 [20.7281, 20.7621]	0.8	20.7587 ± 0.0217 [20.716, 20.801]	0.2	20.7468 ± 0.0087 [20.7298, 20.7637]	0.7
$A_{\text{FB}}^{0,\ell}$	0.0171 ± 0.0010	0.016300 ± 0.000095 [0.016111, 0.016487]	0.016291 ± 0.000096 [0.016102, 0.016480]	0.8	0.016316 ± 0.000240 [0.01585, 0.01679]	0.8	0.01615 ± 0.00011 [0.01594, 0.01636]	1.0
\mathcal{A}_ℓ (SLD)	0.1513 ± 0.0021	0.14742 ± 0.00044 [0.14656, 0.14827]	0.14745 ± 0.00045 [0.14656, 0.14834]	1.8	0.14750 ± 0.00108 [0.1454, 0.1496]	1.6	0.14675 ± 0.00049 [0.14580, 0.14770]	2.1
R_b^0	0.21629 ± 0.00066	0.215892 ± 0.000100 [0.215696, 0.216089]	0.215886 ± 0.000102 [0.215688, 0.216086]	0.6	0.215413 ± 0.000364 [0.21469, 0.21611]	1.2	0.21591 ± 0.00010 [0.21571, 0.21611]	0.6
R_c^0	0.1721 ± 0.0030	0.172198 ± 0.000054 [0.172093, 0.172302]	0.172197 ± 0.000054 [0.172094, 0.172303]	-0.1	0.172404 ± 0.000183 [0.17206, 0.17278]	-0.1	0.172189 ± 0.000054 [0.172084, 0.172295]	-0.1
$A_{\text{FB}}^{0,b}$	0.0996 ± 0.0016	0.10335 ± 0.00030 [0.10276, 0.10396]	0.10337 ± 0.00032 [0.10275, 0.10400]	-2.3	0.10338 ± 0.00077 [0.10189, 0.10490]	-2.1	0.10288 ± 0.00034 [0.10220, 0.10354]	-2.0
$A_{\text{FB}}^{0,c}$	0.0707 ± 0.0035	0.07385 ± 0.00023 [0.07341, 0.07430]	0.07387 ± 0.00023 [0.07341, 0.07434]	-0.9	0.07392 ± 0.00059 [0.07275, 0.07507]	-0.9	0.07348 ± 0.00025 [0.07298, 0.07398]	-0.8
\mathcal{A}_b	0.923 ± 0.020	0.934770 ± 0.000039 [0.934693, 0.934847]	0.934772 ± 0.000040 [0.934693, 0.934849]	-0.6	0.934593 ± 0.000166 [0.93426, 0.93491]	-0.6	0.934721 ± 0.000041 [0.934642, 0.934801]	-0.6
\mathcal{A}_c	0.670 ± 0.027	0.66796 ± 0.00021 [0.66754, 0.66838]	0.66797 ± 0.00021 [0.66755, 0.66839]	0.1	0.66817 ± 0.00054 [0.66712, 0.66922]	0.1	0.66766 ± 0.00022 [0.66722, 0.66810]	0.1
\mathcal{A}_s	0.895 ± 0.091	0.935678 ± 0.000039 [0.935600, 0.935755]	0.935677 ± 0.000040 [0.935599, 0.935754]	-0.4	0.935716 ± 0.000098 [0.935523, 0.935909]	-0.5	0.935621 ± 0.000041 [0.935541, 0.935702]	-0.5
$\text{BR}_{W \rightarrow \ell \bar{\nu}_\ell}$	0.10860 ± 0.00090	0.108388 ± 0.000022 [0.108345, 0.108431]	0.108388 ± 0.000022 [0.108345, 0.108431]	0.2	0.108291 ± 0.000109 [0.10808, 0.10851]	0.3	0.108386 ± 0.000023 [0.108340, 0.108432]	0.2
$\sin^2 \theta_{\text{eff}}^{\text{lept}}(\text{HC})$	0.23143 ± 0.00025	0.231471 ± 0.000055 [0.231362, 0.231580]	0.231474 ± 0.000056 [0.231363, 0.231584]	-0.2	0.231460 ± 0.000138 [0.23119, 0.23173]	-0.1	0.231558 ± 0.000062 [0.231436, 0.231679]	-0.5
R_{uc}	0.1660 ± 0.0090	0.172220 ± 0.000031 [0.172159, 0.172282]	0.172220 ± 0.000032 [0.172159, 0.172282]	-0.7	0.172424 ± 0.000180 [0.17209, 0.17279]	-0.7	0.172212 ± 0.000032 [0.172149, 0.172275]	-0.7

TABLE II. Experimental data, Posterior from the full fit, Indirect determination of individual SM parameters/Prediction of individual EWPO, Full Indirect determination of all SM parameters simultaneously, and Full Prediction of all EWPO simultaneously in the *standard average* scenario. The (Full) Indirect determination/(Full) Prediction is obtained omitting the experimental information on individual (all) SM parameters/individual (all) EWPO.

be tested by looking at the distribution of p -values. From Table II, in the indirect determination case, we find an average p -value of 0.43 with a 0.36 standard deviation, while for the full prediction we obtain an average p -value of 0.56 with a 0.30 standard deviation. Both values are compatible with the expectation of a flatly distributed p -value between zero and one. Furthermore, we evaluate the global p -value from the full prediction, taking into account all theoretical and experimental correlations. We

obtain $p = 2.45 \cdot 10^{-5}$, corresponding to a global pull of 4.2σ , in the *standard* averaging scenario, and $p = 0.10$, corresponding to a global pull of 1.6σ , in the *conservative* averaging scenario.

In view of the significant discrepancy between the SM prediction and the experimental average for M_W , we discuss next the implications of the new Tevatron result on scenarios of NP beyond the SM. In particular we discuss the case of NP models which mainly introduce sizable

EW *oblique* corrections (here denoted as *oblique* models) and the case in which NP is described at the EW scale by more general effective interactions, taking as prototype example the dimension-six SM Effective Field Theory (SMEFT). Let us first consider a class of NP models in which the dominant contributions to EWPO are expected to arise as oblique corrections, i.e. via modifications of the EW gauge-boson self energies, and can thus be parameterized in terms of the S , T , and U parameters introduced in Ref. [47, 48] (or equivalently by the $\varepsilon_{1,2,3}$ parameters introduced in refs. [49–51], although, for the sake of brevity, we consider here only the former set of parameters). The explicit dependence of the EWPO on S , T , and U can be found in appendix A of Ref. [52]. If one assumes NP contributions to U to be negligible, then a prediction for M_W can be obtained from all other EWPO, as reported in Table I, and could reduce the SM discrepancy with the experimental value of M_W to a tension at the 1.5σ level. This scenario, $U \ll S, T$, is expected in extensions with heavy new physics where the SM gauge symmetries are realized linearly in the light fields, in which case U is generated by interactions of mass dimension eight, and is then suppressed with respect to S and T , which are given by dimension-six interactions. Alternatively, to describe scenarios where sizable contributions to U are generated, we also consider the case where this parameter is left free.⁴ In this case, since U is only very loosely constrained by Γ_W , M_W cannot be predicted with a reasonable accuracy. At the same time, this means that the apparent discrepancy with the new M_W measurement can be solved by a nonvanishing U parameter. In Tables III and VII we report the results of a global fit, including M_W , for the oblique parameters, while the corresponding probability density functions (p.d.f.) are presented in Figs. 2 and 4. We also report the value of the *Information Criterion* (IC) [54] of the fits, compared to the SM one. The posterior for the EWPO is reported in Tables IV and IX.

	Result	Correlation	Result	Correlation
	(IC _{ST} /IC _{SM} = 25.0/80.2)		(IC _{STU} /IC _{SM} = 25.3/80.2)	
S	0.100 ± 0.073	1.00	0.005 ± 0.096	1.00
T	0.202 ± 0.056	0.93	0.040 ± 0.120	0.91
U	–	–	0.134 ± 0.087	–0.65 –0.88

TABLE III. Results of the global fit of the oblique parameters to all EWPO in the *standard average* scenario.

We then relax the assumption of dominant oblique NP contributions and consider generic heavy NP within the formalism of the dimension-six SMEFT. Here we work in the so-called *Warsaw basis* [55] assuming fermion universality and, as in the fits presented above, we use the

$\{\alpha, G_\mu, M_Z\}$ EW input scheme [56]. In the Warsaw basis, there are a total of ten operators that can modify the EWPO at leading order, but only eight combinations of the corresponding Wilson coefficients can be constrained by the data in Table II [57, 58]. Using the notation of [55], these combinations can be written as, e.g. [57]

$$\hat{C}_{\varphi f}^{(1)} = C_{\varphi f}^{(1)} - \frac{Y_f}{2} C_{\varphi D}, \quad f = l, q, e, u, d, \quad (6)$$

$$\hat{C}_{\varphi f}^{(3)} = C_{\varphi f}^{(3)} + \frac{c_w^2}{4s_w^2} C_{\varphi D} + \frac{c_w}{s_w} C_{\varphi WB}, \quad f = l, q, \quad (7)$$

$$\hat{C}_U = \frac{1}{2}((C_U)_{1221} + (C_U)_{2112}) = (C_U)_{1221}, \quad (8)$$

where s_w , c_w are the sine and cosine of the weak mixing angle, Y_f denotes the fermion hypercharge and we have absorbed the dependence on the cut-off scale of the SMEFT, Λ , in the Wilson coefficients, i.e. the above coefficients carry dimension of $[\text{mass}]^{-2}$. Furthermore, the effective EW fermion couplings always depend on \hat{C}_U via the following combinations, fixed by the corresponding fermionic quantum numbers (see e.g. [59]),

$$\hat{C}_{\varphi f}^{(3)} - \frac{c_w^2}{2s_w^2} \hat{C}_U \quad \text{and} \quad \hat{C}_{\varphi f}^{(1)} + Y_f \hat{C}_U, \quad (9)$$

such that the effects of \hat{C}_U cannot be separated from other operators using only Z -pole observables. The flat direction can be broken by the W -boson mass, which depends on $\hat{C}_{\varphi l}^{(3)} - \hat{C}_U/2$, or any observable sensitive to its value, e.g. the W -boson width Γ_W . The comparatively low precision of the experimental measurement of Γ_W ($\sim 2\%$) thus results in a weak prediction for M_W from the SMEFT fit, with an uncertainty somewhat below 2 GeV⁵, see Table I, which can easily fit the experimental measurement, via a non-zero value of the combination $\hat{C}_{\varphi l}^{(3)} - \hat{C}_U/2$. Indeed, as can be seen in Tables V and VIII for the standard and conservative scenarios, respectively, the two operators involved in the combination are strongly correlated between them, but also with $\hat{C}_{\varphi l}^{(1)}$. The latter correlation can be understood from the fact that the combination $\hat{C}_{\varphi l}^{(1)} + \hat{C}_{\varphi l}^{(3)}$ is the one that directly corrects the left-handed electron couplings, which is measured to the permil level. The extraction of this coupling from data, however, is typically correlated with the one on the right-handed coupling, sensitive to $\hat{C}_{\varphi e}$, complicating slightly more the correlation pattern in the output of the global fit. It is, in fact, in the information of the leptonic operators where one observes the main difference between the fits using the standard and conservative averages of the experimental values. This is reflected in

⁴ The STU results can also be used to derive constraints in terms of the three combinations of four dimension-six *oblique* operators that affect EWPO, namely S, T, W , and Y [53], via their relation with the $\varepsilon_{1,2,3}$ parameters [53].

⁵ This only accounts for the SMEFT parametric and SM intrinsic uncertainties but neglects the uncertainty associated to higher-order effects in the SMEFT, e.g. from dimension-eight contributions, which could be evaluated via the methods of [60].

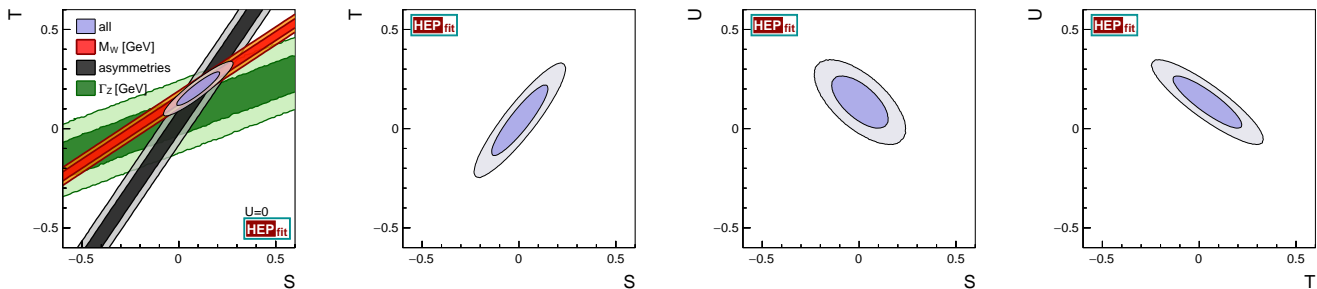


FIG. 2. P.d.f.'s for oblique parameters from a global fit to all EWPO for the *standard average* scenario. (Left panel) Scenario with $U = 0$. (Center and right panels) Scenario with $U \neq 0$. Dark (light) regions correspond to 68% (95%) probability ranges.

	Measurement	ST	STU	SMEFT
M_W [GeV]	80.4133 ± 0.0080	80.4100 ± 0.0077	80.4133 ± 0.0080	80.4133 ± 0.0080
Γ_W [GeV]	2.085 ± 0.042	2.09214 ± 0.00072	2.09251 ± 0.00075	2.0778 ± 0.0070
$\sin^2 \theta_{\text{eff}}^{\text{lept}} (Q_{\text{FB}}^{\text{had}})$	0.2324 ± 0.0012	0.23142 ± 0.00013	0.23147 ± 0.00014	–
$P_{\tau}^{\text{pol}} = \mathcal{A}_{\ell}$	0.1465 ± 0.0033	0.1478 ± 0.0011	0.1474 ± 0.0011	0.1488 ± 0.0014
Γ_Z [GeV]	2.4955 ± 0.0023	2.49812 ± 0.00099	2.4951 ± 0.0022	2.4955 ± 0.0023
σ_h^0 [nb]	41.480 ± 0.033	41.4910 ± 0.0077	41.4905 ± 0.0077	41.481 ± 0.032
R_{ℓ}^0	20.767 ± 0.025	20.7506 ± 0.0084	20.7510 ± 0.0084	20.769 ± 0.024
$A_{\text{FB}}^{0,\ell}$	0.0171 ± 0.0010	0.01638 ± 0.00023	0.01630 ± 0.00024	0.01659 ± 0.00032
\mathcal{A}_{ℓ} (SLD)	0.1513 ± 0.0021	0.1478 ± 0.0011	0.1474 ± 0.0011	0.1488 ± 0.0014
R_b^0	0.21629 ± 0.00066	0.21591 ± 0.00010	0.21591 ± 0.00010	0.21632 ± 0.00065
R_c^0	0.1721 ± 0.0030	0.172198 ± 0.000054	0.172200 ± 0.000054	0.17159 ± 0.00099
$A_{\text{FB}}^{0,b}$	0.0996 ± 0.0016	0.10362 ± 0.00075	0.10336 ± 0.00077	0.1008 ± 0.0014
$A_{\text{FB}}^{0,c}$	0.0707 ± 0.0035	0.07407 ± 0.00058	0.07387 ± 0.00059	0.0734 ± 0.0022
\mathcal{A}_b	0.923 ± 0.020	0.934812 ± 0.000097	0.934779 ± 0.000099	0.903 ± 0.013
\mathcal{A}_c	0.670 ± 0.027	0.66815 ± 0.00052	0.66796 ± 0.00053	0.658 ± 0.020
\mathcal{A}_s	0.895 ± 0.091	0.935710 ± 0.000096	0.935676 ± 0.000097	0.905 ± 0.012
$\text{BR}_{W \rightarrow \ell \bar{\nu}_{\ell}}$	0.10860 ± 0.00090	0.108386 ± 0.000022	0.108380 ± 0.000022	0.10900 ± 0.00038
$\sin^2 \theta_{\text{eff}}^{\text{lept}} (\text{HC})$	0.23143 ± 0.00025	0.23142 ± 0.00013	0.23147 ± 0.00014	–
R_{uc}	0.1660 ± 0.0090	0.172220 ± 0.000032	0.172222 ± 0.000032	0.17161 ± 0.00098

TABLE IV. Posterior distributions for the global fit to all EWPO in the NP scenarios discussed in the text. For the reader's convenience we also report experimental data in the first column. The measurements interpreted as determinations of the effective leptonic weak mixing angle, namely $\sin^2 \theta_{\text{eff}}^{\text{lept}} (Q_{\text{FB}}^{\text{had}})$ and $\sin^2 \theta_{\text{eff}}^{\text{lept}} (\text{HC})$, are not included in the SMEFT fits.

changes in their correlations as well as mild changes, of order ten percent, in their uncertainties, whereas the central values of the Wilson coefficients stay approximately the same. The posterior for the EWPO in this case is also reported in Tables IV and IX.

In conclusion, recent measurements of m_t [1] and M_W [2] are introducing some tensions in global fits of EW precision observables. In this Letter we have studied their impact on electroweak precision fits both in the SM and in some prototype scenarios of NP beyond the SM. Future EW precision measurements at both the LHC and the HL-LHC will add to this picture and contribute to confirm or resolve potential tensions in the SM.

ACKNOWLEDGEMENTS

This work was supported in part by the Italian Ministry of Research (MIUR) under grant PRIN

20172LNEEZ. The work of J.B. has been supported by the FEDER/Junta de Andalucía project grant P18-FRJ-3735. The work of L.R. has been supported by the U.S. Department of Energy under grant DE-SC0010102.

APPENDIX ON THE CONSERVATIVE AVERAGE SCENARIO

In this appendix we present the results of our analysis in the *conservative average* scenario for m_t and M_W . Figure 3 presents the posteriors for different fits in the m_t vs M_W and $\sin^2 \theta_{\text{eff}}^{\text{lept}}$ vs M_W planes in the SM. Results of SM fits are reported in Table VI, while Figure 4 and Table VII present results obtained in the scenario with dominant oblique NP contributions, and Table VIII presents the corresponding results for the SMEFT. Posteriors for all EWPO in the NP scenarios considered are reported in Table IX.

	Result	Correlation Matrix							
		$(IC_{\text{SMEFT}}/IC_{\text{SM}} = 31.8/80.2)$							
$\hat{C}_{\varphi l}^{(1)}$	-0.007 ± 0.011	1.00							
$\hat{C}_{\varphi l}^{(3)}$	-0.042 ± 0.015	-0.68	1.00						
$\hat{C}_{\varphi e}$	-0.017 ± 0.009	0.48	0.04	1.00					
$\hat{C}_{\varphi q}^{(1)}$	-0.018 ± 0.044	-0.02	-0.06	-0.13	1.00				
$\hat{C}_{\varphi q}^{(3)}$	-0.113 ± 0.043	-0.03	0.04	-0.16	-0.37	1.00			
$\hat{C}_{\varphi u}$	0.090 ± 0.150	0.06	-0.04	0.04	0.61	-0.77	1.00		
$\hat{C}_{\varphi d}$	-0.630 ± 0.250	-0.13	-0.05	-0.30	0.40	0.58	-0.04	1.00	
\hat{C}_{ll}	-0.022 ± 0.028	-0.80	0.95	-0.10	-0.06	-0.01	-0.04	-0.05	1.00

TABLE V. Results from the dimension-six SMEFT fit in the *standard average* scenario. The values of the Wilson coefficients \hat{C}_i are given in units of TeV^{-2} .

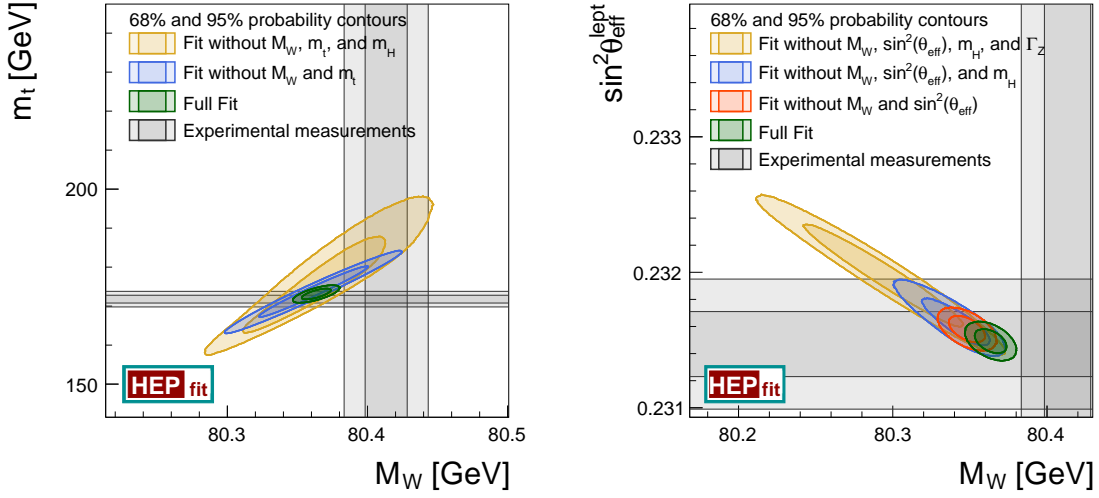


FIG. 3. Same as Figure 1 in the *conservative average* scenario.

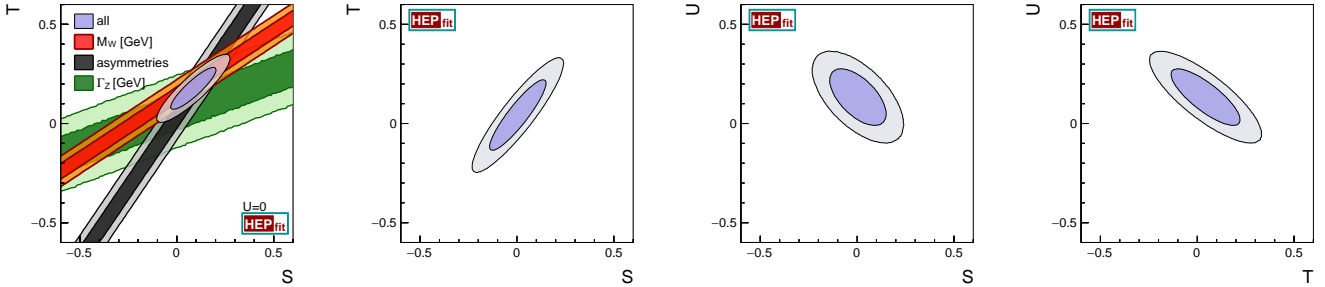


FIG. 4. Same as Figure 2 for the *conservative average* scenario.

	Measurement	Posterior	Indirect/Prediction	Pull	Full Indirect	Pull	Full Prediction	Pull
$\alpha_s(M_Z)$	0.1177 ± 0.0010	0.11786 ± 0.00095 [0.11603, 0.11972]	0.11930 ± 0.00281 [0.11371, 0.12482]	-0.5	0.12174 ± 0.00473 [0.1126, 0.1311]	-0.8	0.1177 ± 0.0010 [0.1157, 0.1197]	-
$\Delta\alpha_{\text{had}}^{(5)}(M_Z)$	0.02766 ± 0.00010	0.027614 ± 0.000097 [0.027422, 0.027804]	0.026895 ± 0.000394 [0.026123, 0.027677]	1.9	0.027987 ± 0.000699 [0.02661, 0.02935]	-0.5	0.02766 ± 0.00010 [0.02747, 0.02786]	-
M_Z [GeV]	91.1875 ± 0.0021	91.1887 ± 0.0021 [91.1847, 91.1927]	91.2227 ± 0.0105 [91.2024, 91.2434]	-3.3	91.2111 ± 0.0390 [91.135, 91.289]	-0.6	91.1875 ± 0.0021 [91.1834, 91.1916]	-
m_t [GeV]	171.8 ± 1.0	173.12 ± 0.92 [171.30, 174.92]	180.10 ± 2.25 [175.66, 184.55]	-3.3	187.16 ± 9.83 [167.9, 206.4]	-1.6	171.8 ± 1.0 [169.8, 173.8]	-
m_H [GeV]	125.21 ± 0.12	125.21 ± 0.12 [124.97, 125.45]	102.19 ± 9.79 [87.01, 127.30]	1.9	245.25 ± 125.35 [98.1, 640.4]	-0.9	125.21 ± 0.12 [124.97, 125.45]	-
M_W [GeV]	80.413 ± 0.015	80.3634 ± 0.0068 [80.3500, 80.3769]	80.3505 ± 0.0077 [80.3355, 80.3655]	3.7	80.4116 ± 0.0146 [80.383, 80.440]	0.0	80.3497 ± 0.0079 [80.3342, 80.3653]	3.7
Γ_W [GeV]	2.085 ± 0.042	2.08859 ± 0.00066 [2.08731, 2.08988]	2.08859 ± 0.00066 [2.08732, 2.08988]	-0.1	2.09426 ± 0.00245 [2.0894, 2.0990]	-0.2	2.08743 ± 0.00073 [2.08601, 2.08889]	0.0
$\sin^2 \theta_{\text{eff}}^{\text{lept}}(Q_{\text{FB}}^{\text{had}})$	0.2324 ± 0.0012	0.231491 ± 0.000059 [0.231376, 0.231608]	0.231490 ± 0.000059 [0.231374, 0.231607]	0.8	0.231461 ± 0.000136 [0.23119, 0.23173]	0.8	0.231558 ± 0.000068 [0.231426, 0.231691]	0.7
$P_\tau^{\text{pol}} = \mathcal{A}_\ell$	0.1465 ± 0.0033	0.14725 ± 0.00046 [0.14634, 0.14817]	0.14727 ± 0.00047 [0.14635, 0.14820]	-0.2	0.14750 ± 0.00108 [0.1454, 0.1496]	-0.3	0.14674 ± 0.00053 [0.14570, 0.14779]	-0.1
Γ_Z [GeV]	2.4955 ± 0.0023	2.49453 ± 0.00066 [2.49324, 2.49584]	2.49434 ± 0.00070 [2.49295, 2.49572]	0.5	2.49528 ± 0.00205 [2.4912, 2.4993]	0.1	2.49396 ± 0.00072 [2.49257, 2.49538]	0.6
σ_h^0 [nb]	41.480 ± 0.033	41.4908 ± 0.0077 [41.4757, 41.5059]	41.4929 ± 0.0080 [41.4772, 41.5087]	-0.4	41.4616 ± 0.0304 [41.402, 41.522]	0.4	41.4924 ± 0.0080 [41.4767, 41.5083]	-0.4
R_ℓ^0	20.767 ± 0.025	20.7491 ± 0.0080 [20.7333, 20.7649]	20.7458 ± 0.0086 [20.7287, 20.7627]	0.8	20.7589 ± 0.0218 [20.716, 20.802]	0.2	20.7470 ± 0.0087 [20.7297, 20.7638]	0.8
$A_{\text{FB}}^{0,\ell}$	0.0171 ± 0.0010	0.01626 ± 0.00010 [0.01606, 0.01647]	0.01625 ± 0.00010 [0.01605, 0.01646]	0.8	0.01631 ± 0.00024 [0.01585, 0.01679]	0.8	0.01615 ± 0.00012 [0.01592, 0.01638]	1.0
\mathcal{A}_ℓ (SLD)	0.1513 ± 0.0021	0.14725 ± 0.00046 [0.14634, 0.14817]	0.14728 ± 0.00049 [0.14632, 0.14824]	1.9	0.14750 ± 0.00108 [0.1454, 0.1496]	1.6	0.14674 ± 0.00053 [0.14570, 0.14779]	2.1
R_b^0	0.21629 ± 0.00066	0.21587 ± 0.00010 [0.21566, 0.21607]	0.21586 ± 0.00011 [0.21565, 0.21607]	0.7	0.21542 ± 0.00037 [0.21467, 0.21613]	1.2	0.21591 ± 0.00011 [0.21570, 0.21611]	0.6
R_c^0	0.1721 ± 0.0030	0.172210 ± 0.000054 [0.172102, 0.172316]	0.172210 ± 0.000054 [0.172103, 0.172317]	0.0	0.172400 ± 0.000185 [0.17205, 0.17277]	-0.1	0.172190 ± 0.000055 [0.172082, 0.172297]	-0.1
$A_{\text{FB}}^{0,b}$	0.0996 ± 0.0016	0.10324 ± 0.00033 [0.10259, 0.10388]	0.10325 ± 0.00035 [0.10258, 0.10393]	-2.2	0.10338 ± 0.00076 [0.10188, 0.10489]	-2.1	0.10287 ± 0.00037 [0.10214, 0.10361]	-2.0
$A_{\text{FB}}^{0,c}$	0.0707 ± 0.0035	0.07377 ± 0.00024 [0.07328, 0.07425]	0.07377 ± 0.00026 [0.07327, 0.07428]	-0.9	0.07391 ± 0.00059 [0.07275, 0.07507]	-0.9	0.07348 ± 0.00028 [0.07293, 0.07403]	-0.8
\mathcal{A}_b	0.923 ± 0.020	0.934746 ± 0.000040 [0.934668, 0.934825]	0.934746 ± 0.000040 [0.934668, 0.934826]	-0.6	0.934594 ± 0.000169 [0.93426, 0.93492]	-0.6	0.934721 ± 0.000041 [0.934640, 0.934802]	-0.6
\mathcal{A}_c	0.670 ± 0.027	0.66789 ± 0.00023 [0.66743, 0.66834]	0.66789 ± 0.00023 [0.66743, 0.66835]	0.1	0.66816 ± 0.00054 [0.66712, 0.66922]	0.1	0.66766 ± 0.00024 [0.66718, 0.66814]	0.1
\mathcal{A}_s	0.895 ± 0.091	0.935663 ± 0.000043 [0.935580, 0.935746]	0.935663 ± 0.000043 [0.935580, 0.935746]	-0.4	0.935714 ± 0.000099 [0.935522, 0.935909]	-0.5	0.935622 ± 0.000045 [0.935533, 0.935709]	-0.5
$\text{BR}_{W \rightarrow \ell \bar{\nu}_\ell}$	0.10860 ± 0.00090	0.108382 ± 0.000022 [0.108339, 0.108425]	0.108382 ± 0.000022 [0.108339, 0.108425]	0.2	0.108293 ± 0.000110 [0.10808, 0.10851]	0.3	0.108386 ± 0.000023 [0.108340, 0.108432]	0.2
$\sin^2 \theta_{\text{eff}}^{\text{lept}}(\text{HC})$	0.23143 ± 0.00025	0.231491 ± 0.000059 [0.231376, 0.231608]	0.231496 ± 0.000061 [0.231376, 0.231616]	-0.2	0.231461 ± 0.000136 [0.23119, 0.23173]	-0.1	0.231558 ± 0.000068 [0.231426, 0.231691]	-0.5
R_{uc}	0.1660 ± 0.0090	0.172231 ± 0.000033 [0.172167, 0.172295]	0.172231 ± 0.000033 [0.172168, 0.172296]	-0.7	0.172424 ± 0.000180 [0.17208, 0.17279]	-0.7	0.172211 ± 0.000034 [0.172145, 0.172277]	-0.7

TABLE VI. Same as Table II in the *conservative average* scenario.

	Result	Correlation	Result	Correlation
	(IC _{ST} /IC _{SM} = 24.5/37.1)		(IC _{STU} /IC _{SM} = 25.3/37.1)	
S	0.086 ± 0.077	1.00	0.004 ± 0.096	1.00
T	0.177 ± 0.070	0.89 1.00	0.040 ± 0.120	0.90 1.00
U	-	- -	0.134 ± 0.095	-0.60 -0.81 1.00

TABLE VII. Same as Table III in the *conservative average* scenario.

	Result	Correlation Matrix							
		(IC _{SMEFT} /IC _{SM} = 32.0/37.1)							
$\hat{C}_{\varphi l}^{(1)}$	-0.007 ± 0.012	1.00							
$\hat{C}_{\varphi l}^{(3)}$	-0.042 ± 0.018	-0.44	1.00						
$\hat{C}_{\varphi e}$	-0.017 ± 0.010	0.52	0.31	1.00					
$\hat{C}_{\varphi q}^{(1)}$	-0.018 ± 0.045	-0.02	-0.05	-0.12	1.00				
$\hat{C}_{\varphi q}^{(3)}$	-0.114 ± 0.044	0.02	0.14	-0.02	-0.36	1.00			
$\hat{C}_{\varphi u}$	0.090 ± 0.150	0.05	-0.04	0.02	0.61	-0.76	1.00		
$\hat{C}_{\varphi d}$	-0.630 ± 0.250	-0.13	-0.04	-0.25	0.40	0.57	-0.04	1.00	
\hat{C}_u	-0.022 ± 0.028	-0.72	0.89	0.01	-0.06	0.03	-0.04	-0.05	1.00

TABLE VIII. Same as Table V for the *conservative average* scenario.

	Measurement	ST	STU	SMEFT
M_W [GeV]	80.413 ± 0.015	80.403 ± 0.013	80.413 ± 0.015	80.413 ± 0.015
Γ_W [GeV]	2.085 ± 0.042	2.0916 ± 0.0011	2.0925 ± 0.0012	2.0778 ± 0.0070
$\sin^2 \theta_{\text{eff}}^{\text{lept}}(Q_{\text{FB}}^{\text{had}})$	0.2324 ± 0.0012	0.23143 ± 0.00014	0.23147 ± 0.00014	–
$P_{\tau}^{\text{pol}} = \mathcal{A}_{\ell}$	0.1465 ± 0.0033	0.1478 ± 0.0011	0.1474 ± 0.0011	0.1488 ± 0.0014
Γ_Z [GeV]	2.4955 ± 0.0023	2.4976 ± 0.0012	2.4951 ± 0.0022	2.4955 ± 0.0023
σ_h^0 [nb]	41.480 ± 0.033	41.4909 ± 0.0077	41.4905 ± 0.0077	41.482 ± 0.033
R_{ℓ}^0	20.767 ± 0.025	20.7507 ± 0.0084	20.7512 ± 0.0084	20.769 ± 0.025
$A_{\text{FB}}^{0,\ell}$	0.0171 ± 0.0010	0.01637 ± 0.00023	0.01630 ± 0.00024	0.01660 ± 0.00032
\mathcal{A}_{ℓ} (SLD)	0.1513 ± 0.0021	0.1478 ± 0.0011	0.1474 ± 0.0011	0.1488 ± 0.0014
R_b^0	0.21629 ± 0.00066	0.21591 ± 0.00011	0.21591 ± 0.00011	0.21632 ± 0.00065
R_c^0	0.1721 ± 0.0030	0.172199 ± 0.000055	0.172199 ± 0.000055	0.17160 ± 0.00099
$A_{\text{FB}}^{0,b}$	0.0996 ± 0.0016	0.10359 ± 0.00075	0.10337 ± 0.00077	0.1009 ± 0.0014
$A_{\text{FB}}^{0,c}$	0.0707 ± 0.0035	0.07403 ± 0.00059	0.07385 ± 0.00059	0.0735 ± 0.0022
\mathcal{A}_b	0.923 ± 0.020	0.934807 ± 0.000097	0.934779 ± 0.000100	0.903 ± 0.013
\mathcal{A}_c	0.670 ± 0.027	0.66811 ± 0.00052	0.66797 ± 0.00053	0.658 ± 0.020
\mathcal{A}_s	0.895 ± 0.091	0.935705 ± 0.000096	0.935677 ± 0.000097	0.905 ± 0.012
$\text{BR}_{W \rightarrow \ell \bar{\nu}_{\ell}}$	0.10860 ± 0.00090	0.108385 ± 0.000022	0.108380 ± 0.000022	0.10900 ± 0.00038
$\sin^2 \theta_{\text{eff}}^{\text{lept}}(\text{HC})$	0.23143 ± 0.00025	0.23143 ± 0.00014	0.23147 ± 0.00014	–
R_{uc}	0.1660 ± 0.0090	0.172221 ± 0.000034	0.172221 ± 0.000034	0.17162 ± 0.00099

TABLE IX. Same as Table IV for the *conservative average* scenario.

- [1] CMS Collaboration, "A profiled likelihood approach to measure the top quark mass in the lepton+jets channel at $\sqrt{s} = 13$ TeV.
- [2] T. Aaltonen *et al.* (CDF), High-precision measurement of the W boson mass with the CDF II detector, *Science* **376**, 170 (2022).
- [3] J. R. Ellis, M. K. Gaillard, D. V. Nanopoulos, and S. Rudaz, The Phenomenology of the Next Left-Handed Quarks, *Nucl. Phys. B* **131**, 285 (1977), [Erratum: *Nucl.Phys.B* 132, 541 (1978)].
- [4] A. J. Buras and M. K. Harlander, A Top quark story: Quark mixing, CP violation and rare decays in the standard model, *Adv. Ser. Direct. High Energy Phys.* **10**, 58 (1992).
- [5] J. de Blas, M. Ciuchini, E. Franco, A. Goncalves, S. Mishima, M. Pierini, L. Reina, and L. Silvestrini, Global analysis of electroweak data in the Standard Model (2021), arXiv:2112.07274 [hep-ph].
- [6] J. de Blas *et al.*, **HEPfit**: a code for the combination of indirect and direct constraints on high energy physics models, *Eur. Phys. J. C* **80**, 456 (2020), arXiv:1910.14012 [hep-ph].
- [7] A. Sirlin, Radiative corrections in the $SU(2)_L \times U(1)$ theory: A simple renormalization framework, *Phys.Rev.* **D22**, 971 (1980).
- [8] W. Marciano and A. Sirlin, Radiative corrections to neutrino induced neutral current phenomena in the $SU(2)_L \times U(1)$ theory, *Phys.Rev.* **D22**, 2695 (1980).
- [9] A. Djouadi and C. Verzegnassi, Virtual very heavy top effects in LEP/SLC precision measurements, *Phys.Lett.* **B195**, 265 (1987).
- [10] A. Djouadi, $\mathcal{O}(\alpha\alpha_s)$ vacuum polarization functions of the standard model gauge bosons, *Nuovo Cim.* **A100**, 357 (1988).
- [11] B. A. Kniehl, Two-loop corrections to the vacuum polarizations in perturbative QCD, *Nucl.Phys.* **B347**, 86 (1990).
- [12] F. Halzen and B. A. Kniehl, Δr beyond one loop, *Nucl.Phys.* **B353**, 567 (1991).
- [13] B. A. Kniehl and A. Sirlin, Dispersion relations for vacuum polarization functions in electroweak physics, *Nucl.Phys.* **B371**, 141 (1992).
- [14] B. A. Kniehl and A. Sirlin, On the effect of the $t\bar{t}$ threshold on electroweak parameters, *Phys.Rev.* **D47**, 883 (1993).
- [15] R. Barbieri, M. Beccaria, P. Ciafaloni, G. Curci, and A. Vicere, Radiative correction effects of a very heavy top, *Phys.Lett.* **B288**, 95 (1992), arXiv:hep-ph/9205238 [hep-ph].
- [16] R. Barbieri, M. Beccaria, P. Ciafaloni, G. Curci, and A. Vicere, Two-loop heavy top effects in the standard model, *Nucl.Phys.* **B409**, 105 (1993).
- [17] A. Djouadi and P. Gambino, Electroweak gauge bosons selfenergies: Complete QCD corrections, *Phys.Rev.* **D49**, 3499 (1994), arXiv:hep-ph/9309298 [hep-ph].
- [18] J. Fleischer, O. Tarasov, and F. Jegerlehner, Two-loop heavy top corrections to the ρ parameter: A simple formula valid for arbitrary Higgs mass, *Phys.Lett.* **B319**, 249 (1993).
- [19] J. Fleischer, O. Tarasov, and F. Jegerlehner, Two-loop large top mass corrections to electroweak parameters: Analytic results valid for arbitrary Higgs mass, *Phys.Rev.* **D51**, 3820 (1995).
- [20] L. Avdeev, J. Fleischer, S. Mikhailov, and O. Tarasov, $\mathcal{O}(\alpha\alpha_s^2)$ correction to the electroweak ρ parameter, *Phys.Lett.* **B336**, 560 (1994), arXiv:hep-ph/9406363 [hep-ph].
- [21] K. Chetyrkin, J. H. Kuhn, and M. Steinhauser, Corrections of order $\mathcal{O}(G_F M_t^2 \alpha_s^2)$ to the ρ parameter, *Phys.Lett.* **B351**, 331 (1995), arXiv:hep-ph/9502291 [hep-ph].
- [22] K. Chetyrkin, J. H. Kuhn, and M. Steinhauser, QCD corrections from top quark to relations between electroweak parameters to order α_s^2 , *Phys.Rev.Lett.* **75**, 3394 (1995), arXiv:hep-ph/9504413 [hep-ph].
- [23] G. Degrossi, P. Gambino, and A. Vicini, Two-loop heavy top effects on the m_Z - m_W interdependence, *Phys.Lett.* **B383**, 219 (1996), arXiv:hep-ph/9603374 [hep-ph].
- [24] G. Degrossi, P. Gambino, and A. Sirlin, Precise calculation of M_W , $\sin^2 \hat{\theta}_W(M_Z)$, and $\sin^2 \theta_{\text{eff}}^{\text{lept}}$, *Phys.Lett.* **B394**, 188 (1997), arXiv:hep-ph/9611363 [hep-ph].
- [25] G. Degrossi and P. Gambino, Two-loop heavy top corrections to the Z^0 boson partial widths, *Nucl.Phys.* **B567**, 3 (2000), arXiv:hep-ph/9905472 [hep-ph].
- [26] A. Freitas, W. Hollik, W. Walter, and G. Weiglein, Complete fermionic two-loop results for the M_W - M_Z interdependence, *Phys.Lett.* **B495**, 338 (2000), arXiv:hep-ph/0007091 [hep-ph].
- [27] J. van der Bij, K. Chetyrkin, M. Faisst, G. Jikia, and T. Seidensticker, Three-loop leading top mass contributions to the ρ parameter, *Phys.Lett.* **B498**, 156 (2001), arXiv:hep-ph/0011373 [hep-ph].
- [28] A. Freitas, W. Hollik, W. Walter, and G. Weiglein, Electroweak two-loop corrections to the M_W - M_Z mass correlation in the standard model, *Nucl.Phys.* **B632**, 189 (2002), arXiv:hep-ph/0202131 [hep-ph].
- [29] M. Awramik and M. Czakon, Complete two loop bosonic contributions to the muon lifetime in the standard model, *Phys.Rev.Lett.* **89**, 241801 (2002), arXiv:hep-ph/0208113 [hep-ph].
- [30] A. Onishchenko and O. Veretin, Two-loop bosonic electroweak corrections to the muon lifetime and M_Z - M_W interdependence, *Phys.Lett.* **B551**, 111 (2003), arXiv:hep-ph/0209010 [hep-ph].
- [31] M. Awramik, M. Czakon, A. Onishchenko, and O. Veretin, Bosonic corrections to Δr at the two loop level, *Phys.Rev.* **D68**, 053004 (2003), arXiv:hep-ph/0209084 [hep-ph].
- [32] M. Awramik and M. Czakon, Two loop electroweak bosonic corrections to the muon decay lifetime, *Nucl.Phys.Proc.Suppl.* **116**, 238 (2003), arXiv:hep-ph/0211041 [hep-ph].
- [33] M. Awramik and M. Czakon, Complete two loop electroweak contributions to the muon lifetime in the standard model, *Phys.Lett.* **B568**, 48 (2003), arXiv:hep-ph/0305248 [hep-ph].
- [34] M. Awramik, M. Czakon, A. Freitas, and G. Weiglein, Precise prediction for the W boson mass in the standard model, *Phys.Rev.* **D69**, 053006 (2004), arXiv:hep-ph/0311148 [hep-ph].
- [35] M. Faisst, J. H. Kuhn, T. Seidensticker, and O. Veretin, Three loop top quark contributions to the rho parameter,

- Nucl. Phys. **B665**, 649 (2003), arXiv:hep-ph/0302275 [hep-ph].
- [36] I. Dubovyk, A. Freitas, J. Gluza, T. Riemann, and J. Usovitsch, The two-loop electroweak bosonic corrections to $\sin^2 \theta_{\text{eff}}^b$, Phys. Lett. B **762**, 184 (2016), arXiv:1607.08375 [hep-ph].
- [37] I. Dubovyk, A. Freitas, J. Gluza, T. Riemann, and J. Usovitsch, Complete electroweak two-loop corrections to Z boson production and decay, Phys. Lett. B **783**, 86 (2018), arXiv:1804.10236 [hep-ph].
- [38] Combination of CDF and D0 results on the mass of the top quark using up 9.7 fb^{-1} at the Tevatron (2016), arXiv:1608.01881 [hep-ex].
- [39] V. Khachatryan *et al.* (CMS), Measurement of the top quark mass using proton-proton data at $\sqrt{s} = 7$ and 8 TeV, Phys. Rev. D **93**, 072004 (2016), arXiv:1509.04044 [hep-ex].
- [40] M. Aaboud *et al.* (ATLAS), Measurement of the top quark mass in the $t\bar{t} \rightarrow \text{lepton} + \text{jets}$ channel from $\sqrt{s} = 8$ TeV ATLAS data and combination with previous results, Eur. Phys. J. C **79**, 290 (2019), arXiv:1810.01772 [hep-ex].
- [41] A. M. Sirunyan *et al.* (CMS), Measurement of the $t\bar{t}$ production cross section, the top quark mass, and the strong coupling constant using dilepton events in pp collisions at $\sqrt{s} = 13$ TeV, Eur. Phys. J. C **79**, 368 (2019), arXiv:1812.10505 [hep-ex].
- [42] A. M. Sirunyan *et al.* (CMS), Measurement of the top quark mass in the all-jets final state at $\sqrt{s} = 13$ TeV and combination with the lepton+jets channel, Eur. Phys. J. C **79**, 313 (2019), arXiv:1812.10534 [hep-ex].
- [43] A. Tumasyan *et al.* (CMS), Measurement of the top quark mass using events with a single reconstructed top quark in pp collisions at $\sqrt{s} = 13$ TeV, JHEP **12**, 161, arXiv:2108.10407 [hep-ex].
- [44] Measurement of the top quark mass using a leptonic invariant mass in pp collisions at $\sqrt{s} = 13$ TeV with the ATLAS detector (2019), ATLAS-CONF-2019-046.
- [45] M. Aaboud *et al.* (ATLAS), Measurement of the W-boson mass in pp collisions at $\sqrt{s} = 7$ TeV with the ATLAS detector, Eur. Phys. J. C **78**, 110 (2018), [Erratum: Eur.Phys.J.C 78, 898 (2018)], arXiv:1701.07240 [hep-ex].
- [46] R. Aaij *et al.* (LHCb), Measurement of the W boson mass, JHEP **01**, 036, arXiv:2109.01113 [hep-ex].
- [47] M. E. Peskin and T. Takeuchi, A new constraint on a strongly interacting Higgs sector, Phys.Rev.Lett. **65**, 964 (1990).
- [48] M. E. Peskin and T. Takeuchi, Estimation of oblique electroweak corrections, Phys.Rev. **D46**, 381 (1992).
- [49] G. Altarelli and R. Barbieri, Vacuum polarization effects of new physics on electroweak processes, Phys. Lett. **B253**, 161 (1991).
- [50] G. Altarelli, R. Barbieri, and S. Jadach, Toward a model independent analysis of electroweak data, Nucl. Phys. **B369**, 3 (1992), [Erratum: Nucl. Phys.B376,444(1992)].
- [51] G. Altarelli, R. Barbieri, and F. Caravaglios, Nonstandard analysis of electroweak precision data, Nucl.Phys. **B405**, 3 (1993).
- [52] M. Ciuchini, E. Franco, S. Mishima, and L. Silvestrini, Electroweak Precision Observables, New Physics and the Nature of a 126 GeV Higgs Boson, JHEP **08**, 106, arXiv:1306.4644 [hep-ph].
- [53] R. Barbieri, A. Pomarol, R. Rattazzi, and A. Strumia, Electroweak symmetry breaking after LEP-1 and LEP-2, Nucl. Phys. B **703**, 127 (2004), arXiv:hep-ph/0405040.
- [54] T. Ando, Predictive bayesian model selection, American Journal of Mathematical and Management Sciences **31**, 13 (2011), <http://dx.doi.org/10.1080/01966324.2011.10737798>.
- [55] B. Grzadkowski, M. Iskrzynski, M. Misiak, and J. Rosiek, Dimension-Six Terms in the Standard Model Lagrangian, JHEP **10**, 085, arXiv:1008.4884 [hep-ph].
- [56] I. Brivio, S. Dawson, J. de Blas, G. Durieux, P. Savard, A. Denner, A. Freitas, C. Hays, B. Pecjak, and A. Vicini, Electroweak input parameters (2021), arXiv:2111.12515 [hep-ph].
- [57] A. Falkowski and F. Riva, Model-independent precision constraints on dimension-6 operators, JHEP **02**, 039, arXiv:1411.0669 [hep-ph].
- [58] I. Brivio and M. Trott, Scheming in the SMEFT... and a reparameterization invariance!, JHEP **07**, 148, [Addendum: JHEP 05, 136 (2018)], arXiv:1701.06424 [hep-ph].
- [59] A. Azatov *et al.*, Off-shell Higgs Interpretations Task Force: Models and Effective Field Theories Subgroup Report (2022), arXiv:2203.02418 [hep-ph].
- [60] T. Corbett, A. Helset, A. Martin, and M. Trott, EWPD in the SMEFT to dimension eight, JHEP **06**, 076, arXiv:2102.02819 [hep-ph].